Physica Scripta. Vol. 53, 312–316, 1996

Isoelectronic Comparison of the Al-like $3s^23p\ ^2P$–$3s3p^2\ ^4P$ Transitions in the ions P III–Mo XXX

Christer Jupén and Lorenzo J. Curtis*

Department of Physics, University of Lund, S-223 62 Lund, Sweden (EURATOM/NFR Fusion Association)

Received June 18, 1995; accepted August 17, 1995

Abstract

New observations of the $3s^23p\ ^2P$–$3s3p^2\ ^4P$ intercombination transitions in Al-like ions have been made for Cl V from spark spectra recorded at Lund and for Kr XXIV and Mo XXX from spectra obtained at the JET tokamak. The new results have been combined with other identifications of these transitions along the sequence and empirically systematized and compared with theoretical calculations. A set of smoothed and interpolated values for the excitation energies of the $3s3p^2\ ^4P$ levels in P III–Mo XXX is presented.

1. Introduction

Until recently, experimental data for the $3s^23p\ ^2P$–$3s3p^2\ ^4P$ intercombination transition for Al-like ions were available only for the lightest elements of the sequence. Träbert *et al.* [1–3], who utilized the beam-foil light source (see Ref. [4]) for identification of intercombination lines, greatly extended the observations along this sequence. In the first of these experiments, nearly all of the five possible transitions of the $3s^23p\ ^2P$–$3s3p^2\ ^4P$ multiplet were identified in Ti X, Fe XIV, Ni XVI and Cu XVII with a wavelength accuracy of about 0.2 Å. For Fe XIV the identifications were corroborated by the same authors [2] using the solar flare spectrum of Dere [5] (wavelength uncertainty ± 0.03 Å). The wavelength uncertainty of these Fe XIV lines was further reduced by tokamak measurements [6]. A summary of all Al-like $3s^23p\ ^2P$–$3s3p^2\ ^4P$ intercombination lines from Ti X to Zn XVIII observed by beam-foil spectroscopy is given in Ref. [3]. Based on this work, Jupén *et al.* [7] identified the $^2P_{3/2}$–$^4P_{3/2}$ and $^2P_{3/2}$–$^4P_{5/2}$ transitions in Kr XXIV from spectra obtained at the JET tokamak.

Using laser-produced plasmas, Ekberg *et al.* [8] have made an isoelectronic investigation of the $3s^23p$, $3p^3$, $3s3p3d$, $3s3p^2$ and $3s^23d$ configurations in Ge XX, Se XXII, Sr XXVI, Y XXVII and Zr XXVIII. Although the high density of the light source did not permit a direct observation of the intercombination lines, the energy levels of the $3s3p^2\ ^4P$ term could be established from other transitions such as $3s3p^2$–$3s3p3d$ and $3s3p^2$–$3p^3$. The three $^2P_{1/2}$–$^4P_{1/2}$, $^2P_{3/2}$–$^4P_{3/2}$ and $^2P_{3/2}$–$^4P_{5/2}$ components in Br XXIII were recently identified by Träbert *et al.* [9] by means of the beam-foil technique. These authors also measured lifetimes of the ^4P levels.

In the present work we report new identifications of the $3s^23p\ ^2P$–$3s3p^2\ ^4P$ transitions in Cl V, Kr XXIV and Mo XXX. These new data, together with previous experimental results, have been compared with theoretical calculations and systematized using empirical mapping reductions and parametrizations. In this way a comprehensive set of isoelectronically smoothed and interpolated $3s3p^2\ ^4P$ excitation energies for P III–Mo XXX were obtained.

2. Experiment

The measurements for Cl V [10] were carried out at Lund using a sliding spark light source operating at 3–15 kV. The light was dispersed by a 3 m normal incidence spectrograph with a scale factor of 2.8 Å/min in first order. Experimental details are given in Ref. [11].

The studies of Kr XXIV and Mo XXX were performed by means of spectra emitted from JET tokamak plasmas. Kr was injected into the plasma using the gas puffing technique and thus under relatively controlled conditions. Mo, on the other hand, was present as an intrinsic impurity. Spectra were recorded in the wavelength region 30–335 Å by means of a 2.0 m XUV grazing incidence spectrometer [12] equipped with a 600 l/mm grating and two microchannel plates coupled to photodiode arrays. Each detector, movable along the Rowland circle, covered a spectral wavelength section of 30–60 Å. Additional details concerning the experimental set-up can be found in Ref. [7].

3. Observations

Our new observations of the $3s^23p\ ^2P$–$3s3p^2\ ^4P$ transitions are presented in Table I. The three identified components in Cl V are accurate to within ± 0.01 Å.

In Kr XXIV we previously [7] identified the $^2P_{3/2}$–$^4P_{5/2}$ and $^2P_{3/2}$–$^4P_{3/2}$ transitions. The latter of these, which was preliminarily given at 272.54 Å, has now been remeasured and changed to 272.56 Å. A spectral section obtained from the JET tokamak ranging from 240 to 290 Å can be seen in Fig. 3 of Ref. [7]. In the previous work [7] we gave a predicted value of the $^2P_{1/2}$–$^4P_{1/2}$ transition at 242.70 Å, which is very close to the Mg-like $3s^2\ ^1S_0$–$3s3p\ ^1P_1$ transition at 242.56 Å [13]. After a closer examination of the spectral region just above the Mg-like line, we found a line at 242.86 Å which we identify as the missing component. Our identification is further supported by an isoelectronic comparison along the sequence. Since the splitting of the $3s^23p\ ^2P$ ground term is accurately know [8, 14], the $^2P_{3/2}$–$^4P_{1/2}$ component could be predicted very well, and it has now been found in the spectra at 318.04 Å.

In Mo XXX we have found the $^2P_{1/2}$–$^4P_{1/2}$ and $^2P_{3/2}$–$^4P_{5/2}$ transitions. The first of these, measured at 185.53 Å, is very close to the $3s^23p^2\ ^3P_1$–$3s3p^3\ ^5S_2$ transition

* Permanent Address, University of Toledo, Toledo, Ohio U.S.A.

Table I. *Identified* $3s^23p\,^2P$–$3s3p^2\,^4P$ *lines of Cl V, Kr XXIV and Mo XXX*

Ion	Intensity[a]	λ (Å)	Transition
Cl V	3	1168.321 ± 0.01	$3s^23p\,^2P_{1/2}$–$3s3p^2\,^4P_{1/2}$
	3	1169.823 ± 0.01	$3s^23p\,^2P_{3/2}$–$3s3p^2\,^4P_{5/2}$
	0	1181.498 ± 0.01	$3s^23p\,^2P_{3/2}$–$3s3p^2\,^4P_{3/2}$
Kr XXIV	60	242.86 ± 0.03	$3s^23p\,^2P_{1/2}$–$3s3p^2\,^4P_{1/2}$
	170	248.07 ± 0.025[b]	$3s^23p\,^2P_{3/2}$–$3s3p^2\,^4P_{5/2}$
	70	272.56 ± 0.03[c]	$3s^23p\,^2P_{3/2}$–$3s3p^2\,^4P_{3/2}$
	50	318.04 ± 0.025	$3s^23p\,^2P_{3/2}$–$3s3p^2\,^4P_{1/2}$
Mo XXX	300 bl Mo XXIX	185.53 ± 0.025	$3s^23p\,^2P_{1/2}$–$3s3p^2\,^4P_{1/2}$
	60	192.26 ± 0.025	$3s^23p\,^2P_{3/2}$–$3s3p^2\,^4P_{5/2}$

[a] The Cl V intensities are visual estimates from photographic plates, whereas the Kr XXIV and Mo XXX intensities are from photometric measurements.

[b] The line has previously been identified by Jupén *et al.* [7].

[c] The line was previously given at 272.54 Å [7] but the measurement has now been improved.

in Si-like Mo XXIX measured at 185.65 Å [15]. The wavelengths of these two lines have been derived by means of the deconvolution program CARATE [16]. This program package fits sums of Gaussian line shapes to the observed spectral structure. The strongest component $^2P_{3/2}$–$^4P_{5/2}$ was found at 192.26 Å. Earlier, these two Mo XXX lines were tentatively given at 186.22 and 195.6 Å by Hinnov *et al.* [17], but at that time the knowledge of the Al sequence was very limited and these tentative identifications are now superseded.

4. Isoelectronic comparisons

Observed data concerning the $3s^23p\,^2P_{1/2}$–$3s3p^2\,^4P_{1/2}$, $3s^23p\,^2P_{3/2}$–$3s3p^2\,^4P_{3/2}$ and $3s^23p\,^2P_{3/2}$–$3s3p^2\,^4P_{5/2}$ transitions are collected in Table II. The values used for ground term fine structure interval $3s^23p\,^2P_{1/2}$–$3s^23p\,^2P_{3/2}$ were taken from Refs [8, 24]. In formulating the isoelectronic systematization of the observed data, attempts were made to find one-to-one mappings that reduce the raw data to a linearized exposition, which can be specified by a number of empirical parameters that is much smaller than the number of data points. It was found that this could be done very effectively by independently considering the quantities *A*, *B* and *C* that are shown schematically in Fig. 1, and correspond to the intervals

$$A \equiv 3s^23p\,^2P_{1/2}\text{–}3s3p^2\,^4P_{1/2}, \quad (1)$$

$$B \equiv 3s3p^2\,^4P_{1/2}\text{–}3s3p^2\,^4P_{3/2}, \quad (2)$$

$$C \equiv 3s3p^2\,^4P_{1/2}\text{–}3s3p^2\,^4P_{5/2}. \quad (3)$$

Also shown schematically in Fig. 1 is a Multiconfiguration Dirac–Fock (MCDF) calculation [18] of interval A, and the fine structure of the ground term (GFS),

$$GFS \equiv 3s^23p\,^3P_{1/2}\text{–}3s^23p\,^2P_{3/2} \quad (4)$$

which has been accurately measured [8, 14], and systematized and smoothed [24] to provide precise recommended values. We found that linear parametrizations could be obtained by considering the difference between A and its MCDF value by considering the difference between GFS and B, and by performing a Sommerfeld screening parameter reduction of the interval C.

Table III lists the observed intervals A, the corresponding MCDF calculations and the difference A-MCDF. This difference is plotted *vs.* $(\alpha Z)^6$ in Fig. 2 and a high degree of linearity is exhibited. A linear fit was made for this exposition, and the smoothed values for A-MCDF obtained from this fit are also presented in Table III. It has been shown [24] that these MCDF calculations [18] possess major deficiencies due to the inadequate inclusion of quantum electrodynamic (QED) corrections and electron correlation, and

Table II. *Base of observed data (in* cm^{-1})

	$3s^23p\,^2P_J$–$3s3p^2\,^4P_{J'}$			
Ion	1/2–1/2 (*A*)	3/2–3/2 (*A* + *B* − GFS)	3/2–5/2 (*A* + *C* − GFS)	Other Refs.
P III	56 921.7 ± 0.5	56 566.9 ± 0.5	56 894.9 ± 0.5	[19]
S IV	71 184.1 ± 0.5	70 574.7 ± 0.5	71 123.3 ± 0.5	[20]
Cl V	85 592.9 ± 1[a]	84 638.3 ± 1[a]	85 483 ± 1[a]	
Ar VI	100 157.2 ± 1	98 748.9 ± 1	99 984 ± 1	[21]
Ti X	160 359 ± 100	155 836 ± 120		[3]
Cr XII	192 001 ± 200	184 843 ± 170	191 110 ± 150	[3]
Mn XIII	208 651 ± 220	199 521 ± 200	207 232 ± 130	[3]
Fe XIV	225 098 ± 15	213 948 ± 8	223 534 ± 8	[3, 6]
Co XV	242 154 ± 120	228 765 ± 45	240 500 ± 90	[3]
Ni XVI	259 471 ± 135	243 546 ± 120	257 255 ± 110	[3]
Cu XVII	276 886 ± 230	258 398 ± 330	274 386 ± 115	[3]
Zn XVIII	295 430 ± 260	273 673 ± 300	291 971 ± 255	[3]
Ge XX	332 671 ± 200	304 131 ± 200	328 106 ± 200	[8]
Se XXII	371 506 ± 200	335 123 ± 200	365 179 ± 200	[8]
Br XXIII	391 236 ± 460	347 947 ± 1800	384 468 ± 450	[9]
Kr XXIV	411 760 ± 50[a]	366 892 ± 35	403 112 ± 40	[7]
Sr XXVI	453 144 ± 200	398 639 ± 200	441 620 ± 200	[8]
Y XXVIII	474 266 ± 200	414 854 ± 200	461 090 ± 200	[8]
Zr XXVIII	495 631 ± 200	431 208 ± 200	480 679 ± 200	[8]
Mo XXX	538 993 ± 70[a]		520 121 ± 70[a]	

[a] This work.

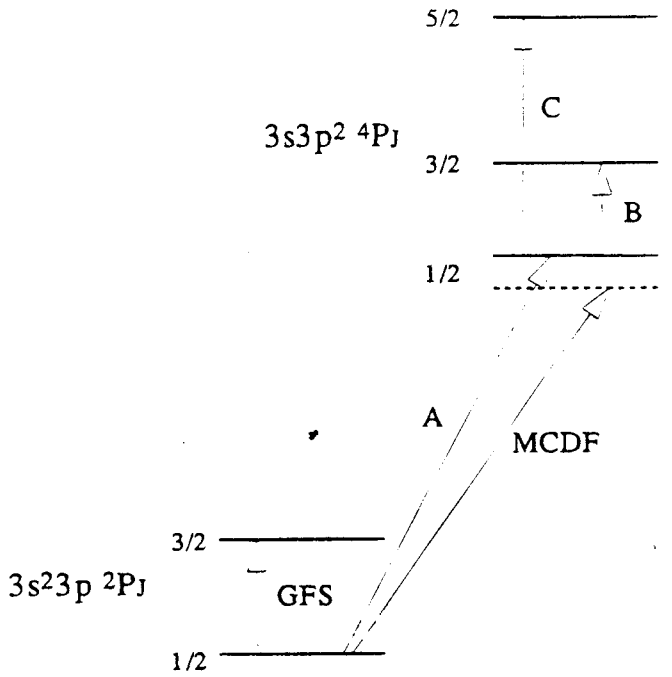

Fig. 1. Energy level diagram indicating the intervals A, B and C, that were parametrized using an MCDF calculation for *A*, the ground term fine structure splitting GFS, and a Sommerfeld screening parameter systematization.

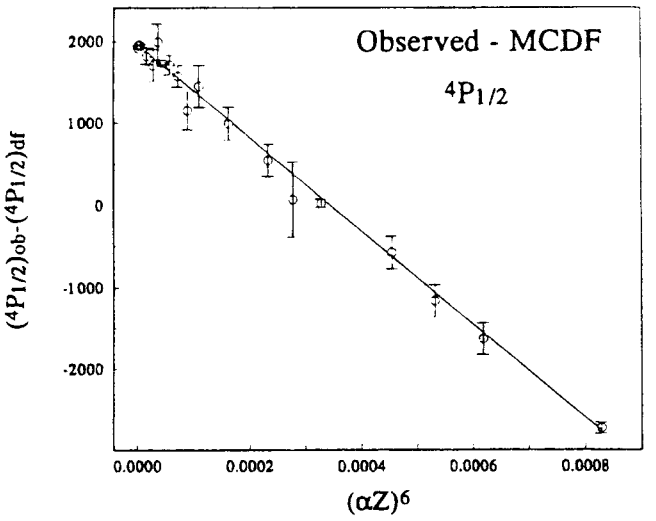

Fig. 2. Plot of the difference between the observed and MCDF values of the interval $3s^2 3p\ ^2P_{1/2}$–$3s3p^2\ ^4P_{1/2}$ *vs.* $(\alpha Z)^6$, indicated by circles with error bars. The solid line traces a linear fit to the data.

Table III. *Smoothed and interpolated values for the* $3s^2 3p\ ^2P_{1/2}$–$3s3p^2\ ^4P_{1/2}$ *intervals based on comparisons between observed and theoretical wavenumbers (in* cm^{-1}*) for ions from P III to Mo XXX*

			A-MCDF	
Ion	MCDF[a]	A (obs)	obs	fit[b]
P III	55 007.0	56 921.7 ± 0.5	1914.7	(1952)[c]
S IV	69 240.8	71 184.1 ± 0.5	1943.3	(1947)[c]
Cl V	83 635.7	85 592.9 ± 1	1957.2	(1942)[c]
Ar VI	98 198.2	100 157.2 ± 1	1959	(1934)[c]
K VII	112 946			1923
Ca VIII	127 903			1910
Sc IX	143 091			1892
Ti X	158 539	160 359 ± 100	1820	1870
V XI	174 272			1843
Cr XII	190 298	192 001 ± 200	1703	1808
Mn XIII	206 660	208 651 ± 220	1991	1766
Fe XIV	223 369	225 098 ± 15	1729	1714
Co XV	240 444	242 154 ± 120	1710	1651
Ni XVI	257 898	259 471 ± 135	1573	1574
Cu XVII	275 738	276 886 ± 230	1148	1483
Zn XVIII	293 983	295 430 ± 260	1447	1374
Ga XIX	312 630			1245
Ge XX	331 679	322 671 ± 200	992	1092
As XXI	351 124			912
Se XXII	370 957	371 506 ± 200	549	701
Br XXIII	391 166	391 236 ± 460	70	455
Kr XXIV	411 734	411 760 ± 50	26	169
Rb XXV	432 649			−164
Sr XXVI	453 721	453 144 ± 200	−557	−550
Y XXVII	475 429	474 266 ± 200	−1163	−996
Zr XXVIII	497 265	495 631 ± 200	−1634	−1511
Nb XXIX	519 368			−2105
Mo XXX	541 719	538 993 ± 70	−2726	−2789

[a] Theoretical calculations by Huang [18].
[b] Fitted to *A*-MCDF = 1964.7 − (13.36 $\alpha Z)^6$.
[c] Uncertainties increased to ±10 cm^{-1} for fitting purposes.

this causes the isoelectronic trends of the calculations to differ substantially from those of observed data. The exposition in Fig. 2 demonstrates convincingly that the deficiencies in this MCDF calculation are dominated by contributions that are proportional to the single power law factor $(\alpha Z)^6$. However, the fact that the trend of the MCDF calculations deviate by thousands of wave numbers on either side of the observed data indicates that they are of limited utility for specifying the fine structure separations. Thus, having used the MCDF calculations to specify the position of the $^4P_{1/2}$ level relative to the ground state, we used purely empirical data-based reductions of the observations to systematize the fine structure of the $3s3p^2\ ^4P$ term.

Table IV lists the difference between the $3s^2 3p\ ^2P_{1/2}$–$3s3p^2\ ^4P_{1/2}$ and $3s^2 3p\ ^2P_{3/2}$–$3s3p^2\ ^4P_{3/2}$ intervals, which corresponds to GFS-B in Fig. 1. It was found that this deficit in the quarted fine structure interval *B* below that of the doublet ground state interval (which possesses the same *J* quantum numbers) had a slower and more regular isoelectronic variation than either B or GFS. This difference is plotted *vs.* $(Z-12)^{5/2}$ in Fig. 3, and here again a high degree of linearity is exhibited. (Notice that an inaccurate and inconsistent point for Br XXIII is clearly revealed.) A linear fit was made to this exposition, and the smoothed values for this difference are also presented in Table IV.

Table V lists the observed values for the interval C, and results of a Sommerfeld screening parameter reduction of this quantity. This involves mapping the observed interval into the effective screening of a hydrogen like term that would have the same splitting. Using a scaled 3p hydrogen like formula, this is of the form

$$C = k\,\frac{R\alpha^2(Z-S)^4}{54}\left[1+\frac{31}{48}\,\alpha^2(Z-S)^2+\cdots\right] \qquad (5)$$

where k is an overall multiplicative scaling factor, adjusted to optimize the regularity of a suitably chosen parametrization of the quantity S. This is a simple mapping of C into S, involving no assumptions, but deriving a utilitarian value from the degree to which it produces a quantity with regular

Table IV. *Smoothed and interpolated values for the differences between the* $3s^23p\,^2P_{1/2}$–$3s3p^2\,^4P_{1/2}$ *and* $3s^23p\,^2P_{3/2}$–$3s3p^2\,^4P_{3/2}$ *intervals (in* cm^{-1}*) for ions from P III to Mo XXX*

Ion	GFS[a]	GFS-*B* (obs)	GFS–B obs	GFS–B fit[b]
P III	559.1	204.8 ± 0.7	354.8	(308)[c]
S IV	952	341.6 ± 0.7	609.4	(563)[c]
Cl V	1492	536.4 ± 0.7	954.6	(934)[c]
Ar VI	2210	798.7 ± 0.7	1408.3	(1436)[c]
K VII	3134			2081
Ca VIII	4308			2879
Sc IX	5761			3843
Ti X	7543	3020 ± 156	4523	4981
V XI	9696			6303
Cr XII	12261			7819
Mn XIII	15295	6165 ± 297	9130	9537
Fe XIV	18852	7701 ± 17	11150	11465
Co XV	22984	9581 ± 128	13389	13610
Ni XVI	27756	11836 ± 180	15925	15982
Cu XVII	33231	14751 ± 402	18488	18586
Zn XVIII	39475	17726 ± 397	21757	21431
Ga XIX	46559			24524
Ge XX	54567	26027 ± 283	28540	27870
As XXI	63550			31477
Se XXII	73626	37243 ± 283	36383	35351
Br XXIII	84846	41560 ± 1858	43289	39498
Kr XXIV	97322	52444 ± 61	44868	43925
Rb XXV	111148			48637
Sr XXVI	126414	71909 ± 283	54505	53641
Y XXVII	143221	83809 ± 283	59412	58942
Zr XXVIII	161680	97257 ± 283	64423	64546
Nb XXIX	181929			70458
Mo XXX	204048			76684

[a] Values taken from Refs [8] and [24].
[b] Fitted to GFS-$B = 65.89 + 15.54(Z - 12)^{5/2}$.
[c] Uncertainties increased to $\pm 10\,cm^{-1}$ for fitting purposes.

Table V. *Smoothed and interpolated values for the* $3s3p^2\,^4P_{1/2}$–$3s3p^2\,^4P_{5/2}$ *intervals (in* cm^{-1}*) obtained from a Sommerfeld screening parametrization for ions from P III up to Mo XXX*

Ion	*C* (obs)	*S* (obs)	*S* (fit)[a]	*C* (fit)[a]
P III	532.4 ± 0.7	6.4070	6.4074	532.1
S IV	890.2 ± 0.7	6.2304	6.2312	889.8
Cl V	1381.1 ± 1.4	6.0988	6.0984	1381.7
Ar VI	2033.8 ± 1.4	5.9939	5.9941	2035.7
K VII			5.9038	2882
Ca VIII			5.8290	3952
Sc IX			5.7658	5283
Ti X			5.7090	6911
V XI			5.6608	8877
Cr XIII			5.6180	11225
Mn XIII	13876 ± 256	5.6342	5.5797	14000
Fe XIV	17287 ± 17	5.5478	5.5446	17250
Co XV	21316 ± 150	5.4565	5.5126	21027
Ni XVI	25545 ± 174	5.4676	5.4832	25386
Cu XVII	30739 ± 257	5.4102	5.4550	30383
Zn XVIII	36024 ± 364	5.4652	5.4318	36079
Ga XIX			5.4090	42537
Ge XX	49999 ± 283	5.3934	5.3947	49824
As XXI			5.3797	58008
Se XXII	67302 ± 283	5.3682	5.3691	67163
Br XXIII	78081 ± 644	5.3003	5.3611	77364
Kr XXIV	88664 ± 64	5.3560	5.3553	88690
Rb XXV			5.3483	101225
Sr XXVI	114876 ± 283	5.3408	5.3415	115055
Y XXVII	130028 ± 283	5.3320	5.3333	130269
Zr XXVIII	146728 ± 283	5.3193	5.3213	146961
Nb XXIX			5.3058	165228
Mo XXX			5.2869	185171

[a] Fitted to eq. (5) with $k = 0.9$ and $S = 4.943 + 12.588/(Z - S)$.

and slowly varying isoelectronic variation. Through a search, the constant k was chosen to be 0.9, in which case a plot of S *vs.* $1/(Z - S)$ yields the exposition shown in Fig. 4. Here, no significant deviations from linearity are discernable (although a similar reduction of the corresponding MCDF [18] calculations for this interval exhibited substantial deviations from linearity). A linear fit was made and the smoothed values of both S and C and the results are listed in Table V.

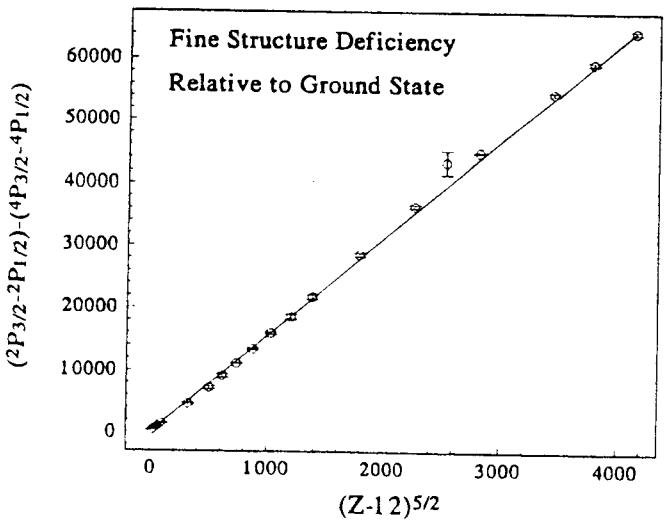

Fig. 3. Plot of the difference between the observed intervals $3s^23p\,^2P_{1/2}$–$3s3p^2\,^4P_{1/2}$ and $3s^23p\,^2P_{3/2}$–$3s3p^2\,^4P_{3/2}$ *vs.* $(\alpha Z)^{5/2}$, indicated by circles with error bars. The solid line traces a linear fit to the data.

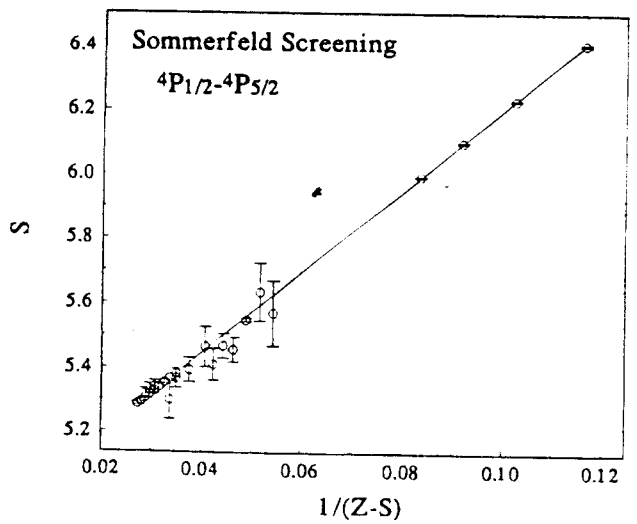

Fig. 4. Screening parametrization of the fine structure interval $3s3p^2\,^4P_{1/2}$–$3s3p^2\,^4P_{5/2}$. S denotes the central screening that a 3p hydrogen like term that would have a scaled fraction (here 90%) of the observed intervals. The observations are denoted by circles with error bars. The solid line traces a linear fit to the data.

Table VI. *Recommended smoothed and interpolated excitation energies (cm^{-1})*

Ion	$3s3p^2\,4P_J$ 1/2	3/2	5/2
P III	56 922[a]	57 126[a]	57 454[a]
S IV	71 184[a]	71 527[a]	72 075[a]
Cl V	85 593[a]	86 130[a]	86 975[a]
Ar VI	100 157[a]	100 959[a]	102 194
K VII	114 869	115 922	117 751
Ca VIII	129 813	131 241	133 765
Sc IX	144 983	146 902	150 266
Ti X	160 409	162 971	167 320
V XI	176 115	179 507	184 992
Cr XII	192 106	196 548	203 331
Mn XIII	208 426	214 184	222 425
Fe XIV	225 083	232 470	242 332
Co XV	242 095	251 468	263 122
Ni XVI	259 472	271 247	284 858
Cu XVII	277 221	291 866	307 604
Zn XVIII	295 357	313 401	331 436
Ga XIX	313 875	335 910	356 412
Ge XX	332 771	359 468	382 595
As XXI	352 036	384 109	410 044
Se XXII	371 658	409 934	438 821
Br XXIII	391 621	436 969	468 985
Kr XXIV	411 903	465 300	500 593
Rb XXV	432 485	494 996	533 710
Sr XXVI	453 171	525 944	568 226
Y XXVII	474 433	558 712	604 702
Zr XXVIII	495 754	592 888	642 715
Nb XXIX	517 263	628 734	682 491
Mo XXX	538 930	666 293	724 101

[a] Observed values have uncertainties $\leqslant 1\,cm^{-1}$ and are tabulated here without smoothing.

Collecting the fitted values, the smoothed values can be generated by use of the empirically determined formulae

$$A = \mathrm{MCDF} + 1964.7 - (13.36\alpha Z)^6, \tag{6}$$

$$B = \mathrm{GFS} - 65.89 - 15.54(Z-12)^{5/2}, \tag{7}$$

$$C = 0.9\,\frac{R\alpha^2(Z-S)^4}{54}\left[1+\frac{31}{48}\,\alpha^2(Z-S)^2\right], \tag{8}$$

$$S = 4.943 + \frac{12.588}{(Z-S)}. \tag{9}$$

Table VI presents the values for the $3s3p^2\,{}^4P$ excitation energies obtained for A, $A+B$ and $A+C$ using eqs (6)–(8).

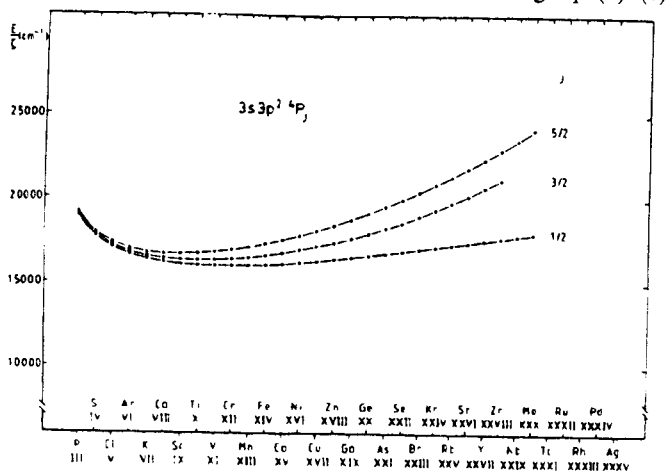

Fig. 5. Isoelectronic comparison of the smoothed values of the observed energy levels of the $3s3p^2\,{}^4P$ divided by the spectrum number.

In the highly ionized atoms the term structure is best described by *jj*-coupling, whereas in the range from the lowest charge states up to the Fe group the *LS* coupling approximation is valid. This is illustrated in Fig. 5, which displays the smoothed data energy levels from Table VI divided by the spectrum number $\zeta = Z - 12$.

5. Conclusion

Through new measurements and data base systematizations we have obtained a smoothed and interpolated set of values for the $3s3p\,{}^4P$ levels in the Al isoelectronic sequence for Al III–Mo XXX. The virtue of this smoothing process does not rely on the fundamental correctness of the mapping functions, but rather on the slow and regular isoelectronic variations that result. This allows accurate interpolations and smoothing, and permits inaccurate and inconsistent data to be identified and critically examined. However, the degree of linearity exibited by Figs 2–4 is so striking that it may suggest the origin of flaws in existing theoretical results and point to large scale trends that can be used to test subsequent calculations.

Acknowledgements

This work has been supported by the European Communities under an association contract between EURATOM and the Swedish Natural Science Research Council, and by the U.S. Department of Energy, Office of Basic Energy Sciences, Division of Chemical Sciences.

References

1. Träbert, E., Hutton, R. and Martinson. I., Z. Phys. **D5**, 125 (1987).
2. Träbert, E., Hutton, R. and Martinson, I., Mon. Not. R. Astron. Soc. **227**, 27 (1987).
3. Träbert, E., Heckmann, P. H., Hutton, R. and Martinson, I., J. Opt. Soc. Am. **B5**, 2173 (1988).
4. Träbert, E., Physica Scripta **48**, 699 (1993).
5. Dere, C., Astrophys. J. **221**, 1062 (1978).
6. Jupén, C., Isler, R. C. and Träbert, E., Mon. Not. R. Astron. Soc. **264**, 627 (1993).
7. Jupén, C., Denne, B. and Martinson, I., Physica Scripta **41**, 669 (1990).
8. Ekberg, J. O., Redfors, A., Brown, C. M., Feldman, U. and Seely, J. F., Physica Scripta **44**, 539 (1991).
9. Träbert, E. *et al.*, Phys. Rev. **A47**, 3805 (1993).
10. Fremberg, J. and Jupén, C., University of Lund, unpublished material.
11. Jupén, C., Fremberg, J. and Fawcett, B., Physica Scripta **30**, 200 (1984).
12. Schwob, J. L., Wouters, A. W., Suckewer, S. and Finkenthal, M., Rev. Sci. Instr. **58**, 1601 (1987).
13. Wyart, J.-F. and TFR Group, Physica Scripta **31**, 539 (1985).
14. Sugar, J., Kaufman, V. and Rowan, W. L., J. Opt. Soc. Am. **B5**, 2183 (1988).
15. Jupén, C., Martinson, I. and Denne-Hinnov, B., Physica Scripta **44**, 562 (1991).
16. Carlén, L., Internal Report LUND 6/(NFFK-7014), University of Lund.
17. Hinnov, E. *et al.*, J. Opt. Soc. Am. **B3**, 1288 (1986).
18. Huang, K.-N., At. Data Nucl. Data Tables **34**, 1 (1986).
19. Magnusson, C. E. and Zetterberg, P. O., Physica Scripta **15**, 237 (1977).
20. Joelsson, I., Engström, L., Magnusson, C. E. and Zetterberg, P. O., J. Phys. Chem. Ref. Data **19**, 844 (1990).
21. Hallin, R., unpublished work quoted by Ekberg, J. O. and Svensson. L. Å., Physica Scripta **2**, 283 (1970).
22. Litzén, U. and Redfors, A., Phys. Lett. **A127**, 88 (1988).
23. Redfors, A. and Litzén, U., J. Opt. Soc. Am. **B6**, 1447 (1989).
24. Kim, Y.-K., Sugar, J., Kaufman, V. and Ali, M. A., J. Opt. Soc. Am. **B10**, 2225 (1988).